Aalborg Universitet

Cable Connection Optimization for Onshore Wind Farms Considering Restricted Area and Topography

Li, Junxian; Hu, Weihao; Wu, Xiawei; Huang, Qi; Liu, Zhou; Chen, Cong; Chen, Zhe

Cable Connection Optimization for Onshore Wind Farms Considering Restricted Area and Topography

Junxian Li, Weihao Hu , *Senior Member, IEEE*, Xiawei Wu, Qi Huang , *Senior Member, IEEE*, Zhou Liu , *Senior Member, IEEE*, Cong Chen, and Zhe Chen , *Fellow, IEEE*

Abstract—For onshore wind farms where all wind turbine (WT) locations are fixed, it is necessary to design corresponding cable connections to collect electricity generated by each WT. The cable connection system should ensure the collection of electricity successfully and reduce the cable cost optimally. Cables are prohibited from crossing restricted land areas, such as reserves, oil wells, and rocky areas. Therefore, in this article, a restricted area is added to the planning area of onshore wind farms. To obtain more accurate final optimized results, we consider topographic factors of onshore wind farms in the optimization process. The algorithm used for cable connection optimization is the dynamic minimum spanning tree. Results indicate the nonnegligible effects of the restricted area and topographic factors on the cable connection topology. The total cable cost savings can exceed 1.8% compared with the reference cable connection topology, in which the topographic factors and restricted area are not considered.

Index Terms—Dynamic minimum spanning tree (DMST), onshore wind farm, restricted area, topographic factors.

NOMENCLATURE

$I_{i,\text{rated}}$	Rated current of cable i.
Q_i	Number of cable in line i.
$U_{i,\text{rated}}$	Rated voltage of cable i.
L_i	Length of cable i.
C_i	Unit price of cable i.
cost_i	Cost of cable i.

I. INTRODUCTION

CURRENTLY, energy crisis and environmental pollution are becoming more serious. Renewable energies have been developed to achieve sustainable development. Wind energy is a popular clean energy and has garnered significant attention recently owing to its abundant resources and significant reduction in greenhouse gas emissions. Because offshore wind energy

Fig. 1. Configuration of onshore wind farm.

is abundant and wind farms are generally large, many wind farms are built at sea. However, with the increased number of offshore wind farms and the effects of adverse weather at sea, areas suitable for the construction of wind farms are becoming fewer. In fact, wind energy captured by onshore wind farms in reasonable designs will not be much lower than that captured by offshore wind farms. In addition, the investment cost for onshore wind farms, including construction, maintenance, installation, and power transmission system (TS) is lower than that for offshore wind farms [1], [2]. Hence, the design of onshore wind farms must be improved.

The electrical system of the entire onshore wind farm comprises two parts: collection system (CS) and TS, as illustrated in Fig. 1. The power production generated by every wind turbine (WT) is transmitted to the substation through medium-voltage cables. The voltage will be adjusted to the appropriate level in a substation. Subsequently, the electric energy is transmitted to a high-voltage substation through a transmission cable, which is expressed as a dotted line in Fig. 1. It is noteworthy that the cables in both the CS and TS must be selected appropriately to satisfy the current-carrying capacity limitations. To satisfy transmission requirements, we should use a smaller cable cross-sectional area and a smaller total cable length to lower the total cable cost. Meanwhile, the cable connection layout in the onshore wind farm is closely related to the substation location. Therefore, a suitable location for building a substation should be determined while optimizing the cable connection to obtain better results.

With the increasing scale of wind farms in recent years, more attention is focused on the effective cable collection and transmission of electrical energy. To effectively integrate direct current (dc) transmission technology for an efficient power transmission, the concepts of dc–dc power conversion and dc WTs have been applied to all-dc wind farms [3]. Considering the present feasibility, the wind farm is not an all-dc wind farm. Additionally, Wang *et al.* [4] proposed an optimal reactive power dispatch strategy to reduce wind farm losses. CSs with multiple structures were compared in [5], where the cable connection was optimized according to the stability and production cost of electricity. After the layout of the onshore wind farm and the number of substations on onshore wind farms have been confirmed, the layout of cables must be optimized to minimize the cable cost. Because the scale of the studied wind farm is extremely large and more than one substation must be built, the fuzzy C-means clustering (FCM) algorithm has been applied in [6]. Using this algorithm, a large-scale wind farm is categorized into several parts. The cluster center of each part is the location of the substation. The WTs and substation of each part are connected by the minimum spanning tree (MST) algorithm. Finally, all substations are connected to form a wind farm power CS. The method of classifying WTs, similar to the FCM algorithm, can reduce the difficulty in optimization. However, the number of clusters is set in advance and the numbers of WTs in each cluster are the same. This classification method may render nonoptimal solutions. The genetic algorithm (GA) was applied in [7] and [8]. In [7], the overall cable length, initial cost, and power losses were considered to obtain a more suitable cable connection layout. In [8], an evolutionary version of the multiple traveling salesman problem based on the GA was proposed as a novel method to optimize cable connections. Results could be obtained in fewer iterations. Unfortunately, crossover occurred in the cable connection layout [7], [8]. If the electrical network on a wind farm is radial or meshed, the algorithm in [9], which combines the GA with a specific algorithm, should be applied as it uses the shortest connection distance between WTs and substations into consideration. The crossover may increase the connection length and consequently increase the total cost. Planar open vehicle routing was applied in [10] to obtain a cable connection layout. However, the performances based on selecting the cable cross-sectional area and clustering of WTs were poor. Hou *et al.* [11] utilized the MST to connect WTs. Using the MST algorithm allows the cable connection layout to avoid cable crossing. The selection of cable type and quantity can be confirmed according to a set containing the number of WTs behind a branch. The overall trenching length is reduced using the MST. To further optimize the length and type of the connection cable, Hou *et al.* [12] utilized the dynamic MST (DMST) algorithm. Mixed integer programming [13], [14] and mixed integer linear programming [15] can be used to optimize wind farm cable connections. The methods presented in [11]–[15] focused on reducing the total trenching length of wind farms to minimize the cable cost. However, the effects of topographic factors on cable length were not considered in [5]–[15]. Moreover, the area reported in [5]–[15] was supposed to be continuously available. However, a landowner may own a piece of land on the wind farm, as reported in [16]. If the cable passes through the land, additional fees will be paid to the owner. In addition, there may be some restricted areas, such as oil wells and rocky areas, on wind farms, these factors are considered in [17] to effectively plan the layout of WTs. However, the effects of these factors on the cable topology were not considered in [17]. In this article, these factors are considered to obtain a better cable topology.

The DMST algorithm is proposed herein to solve CS cable connection problems. The MST can only ensure the minimum cable length, whereas the DMST considers the cable current-carrying capacity and yields the minimum-cost cable connection. The proposed method uses the cable cost as a branch weight to quickly obtain the minimum-cost cable connection and avoid the appearance of cross edges. In this article, the restricted area and topography affect the final optimal cable connection layout by changing the length of related cables. If the planned substation location is extremely close to the WT, the substation position is adjusted in the optimization process of the DMST to reduce the probability of failure on onshore wind farms. This novel method has been performed on an irregular onshore wind farm and a regular onshore wind farm, and the results indicated that the CS layout obtained by the proposed method was more advantageous for onshore wind farms.

This article is organized as follows. To solve the problems posed herein, a few cost models of wind farms and the relevant methods are described in Section II. An irregular onshore wind farm is presented as case study in Section III to illustrate the effects of the restricted area and topography on onshore wind farms. Comparing the results in Scenario III, the conclusions of the DMST based on considering the restricted area and topographic factors are presented in Section IV.

II. METHODOLOGY

In this section, the formulations used for calculating the cable cost, transformer cost, and power losses in cables are provided. Next, the advantages of the DMST compared with the MST are introduced. Subsequently, the location of the substation is analyzed and adjusted until the operation requirements of the onshore wind farm are satisfied. A method using the shortest cable length is proposed while the cable bypasses the restricted area. Herein, it is shown that the effect of topography is reflected better in the change of cable length by comparing the two schemes. Finally, the cross-sectional area of the cable and the optimization framework are shown.

A. Cost Model

The mathematical model in [18] was used to calculate the cable cost. This formula is widely used and shown as follows:

$$C_i = A_p + B_p \exp\left(\frac{C_p S_{n,i}}{10^8}\right)^2 \tag{1}$$

$$S_{n,i} = \sqrt{3} I_{i,\text{rated}} U_{i,\text{rated}}. \tag{2}$$

Here, A_p, B_p, and C_p are the coefficients of the cable cost model, in which their detailed descriptions are available in [16]. The unit cost of the cable (C_i) is based on its rated apparent

This article has been accepted for inclusion in a future issue of this journal. Content is final as presented, with the exception of pagination.

LI *et al.*: CABLE CONNECTION OPTIMIZATION FOR ONSHORE WIND FARMS CONSIDERING RESTRICTED AREA AND TOPOGRAPHY 3

power $(S_{n,i})$, which is closely related to the cross-sectional area of the cable. The cable type should be selected appropriately to satisfy the current-carrying capacity and reduce the cross-sectional area of the cable. With many WTs behind a branch and more than one cable required, the cable cost of this branch can be expressed as

$$\text{cost}_i = Q_i C_i (x, y) L_i (x, y). \tag{3}$$

The CS collects the power production generated by each WT to the substation. The transformer in the substation adjusts the power voltage to the appropriate level and then passes it to the high-voltage substation. The transformer cost in the CS is shown as [19]

$$C_{\text{transformer}} = 0.03327 \times S^{0.7513} \tag{4}$$

where S represents the apparent power of the transformer. Typical transformer apparent power values are listed as follows:

$$S[\text{MVA}] = \{150, 180, 200, 250, 300, 400, 630, 722, 800\}.$$

B. Dynamic Minimum Spanning Tree

The MST algorithm is a vertex connection method in the traditional graph theory. By adapting this algorithm, a minimal subgraph from the original connected graph can be generated. The minimal subgraph has the same number of vertices as the original connected graph, and the total edge weight is the smallest. Based on this idea, the locations of the substation and WTs are regarded as vertices, and the cable length between two WTs are regarded as the branch weight. Subsequently, the CS cable connection layout problem can be converted into the problem of obtaining the MST solution in a weighted graph, expressed as [20]

$$G_T = (V, B_T, W_T) \quad G_T \leq G, B_T \leq B, W_T \leq W \tag{5}$$

where G is the original connected graph, and G_T is the minimal subgraph produced by the MST. V represents the total number of vertices in G. B_T represents all branches in G_T, and W_T is the sum of branch weights in G_T. Currently, two widespread methods can be used to obtain the MST: the Prim and Kruskal algorithms and in this article, the Prim algorithm was used.

After the CS cable connection layout was confirmed, the cable type and number in a branch were determined by the number of WTs connected behind this branch. The MST uses only the total distance between vertices as the objective function to form the final cable connection layout. However, cable costs are related to the type and number of cables among WTs. According to the work in [11], the DMST is an evolutional method of the MST. If a WT is to be added to a spanning tree, the DMST will select the current minimum cost cable connection to connect the WT, i.e., not only the shortest cable as in the MST. Fig. 2 illustrates the advantages of the DMST over the MST in reducing the cable cost.

Fig. 2(a) shows an undirected connected graph comprising eight vertices. The cost of each branch is marked. Point A is regarded as a substation and selected as the starting point for search. The other seven vertices are regarded as WTs. If the MST algorithm is used to connect all WTs to the substation, the final
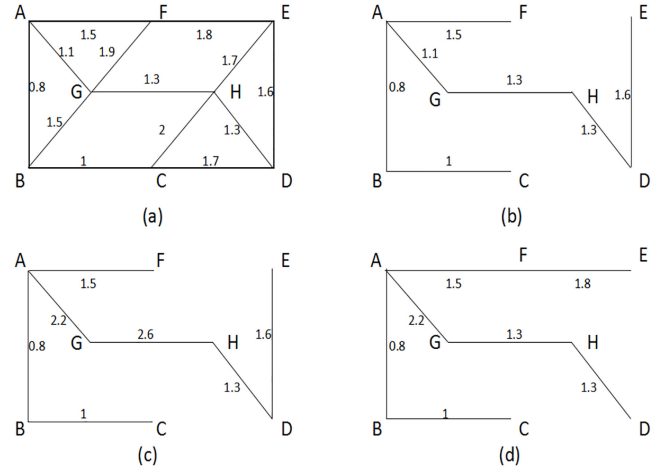

Fig. 2. Comparison of DMST and MST algorithms. (a) Undirected connected graph. (b) Tree generated by MST. (c) Tree generated by MST after changing the weight. (d) Tree generated by DMST after changing the weight.

connection layout is as shown in Fig. 2(b). In this case, the sum of the cost is 8.6. The cable selected for the wind farm must satisfy the current-carrying capacity. Because more than two WTs are connected to a branch, the cost of this branch will double to satisfy the current-carrying capacity. Under this assumption, the cost of each branch of the connection graph obtained by the MST is as shown in Fig. 2(c). The total cost is 11. Fig. 2(d) shows the connection layout obtained by the DMST. In this case, the sum of the cost is 9.9. Comparing Fig. 2(c) and (d), the cost of the connection layout using the DMST is smaller. Therefore, the DMST was used in this study.

Considering the cable cost, the problem can be expressed by the following objective function:

$$\text{Cost}_{\min} = \min \left(\sum_{i=1}^{N-1} C_i^{G_T} L_i^{G_T} \right), G_T \in G \tag{6}$$

where the constraints are as follows:

$$I_i \leq I_{i,\text{rated}}; i \in (1, N-1). \tag{7}$$

To generate a cable connection layout with the DMST, we established five sets and one matrix as follows [21].

Set I: Include vertices appended to the MST.

Set II: Include vertices that have not been appended to the MST.

Set III: Include the weights of branches that were selected to connect the vertices in the MST.

Set IV: Include all WTs connected behind each branch in the MST.

Set V: Include the cross-sectional area of each cable in the MST.

Adjacency matrix: Include all the weights between two vertices. In the optimization process, the weights represent the cost of the branches.

First, Sets I, III, and IV are empty, and Set II includes all the vertices. The location of substation V_1 was selected as the starting point and Set II was transformed to Set I. Subsequently,

the branches connected to V_1 were compared. The branch that expresses the minimum cable cost under the current cable connection will be appended to Set III. The vertex V_1 transformed from Set II to Set I will be deleted from Set II. During the process, the number of WTs connected to a branch is incremented and the corresponding data should be recorded in Set IV. If the number of WTs connected to a certain cable exceeds the capacity limit, the cross-sectional area of the cable in that branch should be updated and recorded in Set V. The process does not end until Set II becomes empty.

C. Optimization of Substation Location

The cable connection in the CS is closely related to the substation location. All points in a planned area were traversed to determine the optimal substation location. By comparing the cost of cable connection in different substation locations, the best substation location can be confirmed. If the initial optimized substation location is extremely close to one WT location, the substation position must be readjusted while considering the safe operation of the wind farm. If the distance between the initial optimized substation location and a WT location is less than two rotor diameters (2D), as shown in Fig. 3(a), then the new optimized substation location is replanned on a circle with the center of the nearest WT and a radius of 2D. Therefore, the distance between the substation and WT satisfies the safety requirements of onshore wind farms, as shown in Fig. 3(b). When readjusting the substation location, restrictions, such as the current-carrying capacity, must be satisfied. The substation location was optimized as follows.

1) Try all possible substation locations. The cable connection layout corresponding to each substation location was obtained by the DMST algorithm. Compare all the results to find the result with the lowest cable cost.
2) After the initial optimal substation location was determined, the distance between it and the nearest WT was calculated.
3) If the distance is larger than 2D, the substation location need not to be adjusted. Otherwise, proceed to step 4).
4) The new optimized substation location was replanned on a circle with the center of the nearest WT and a radius of 2D. Substation location adjustments should only affect the length of the cable directly connected to the substation. Other cable topologies and type choices should not be affected, as shown in Fig. 3(b).

Finally, the security of the system was guaranteed. The adjusted substation location only affected the length of the cable that was directly connected to it. The types of cables in the CS and the length of cables not directly connected to the substation were not affected. Therefore, the final adjusted substation location afforded a relatively low cost of the CS while ensuring the safe operation of the system.

D. Bypassing Restricted Area

On an onshore wind farm, not all land may be available. If an area belonging to a landowner is occupied by an onshore wind farm, additional compensation is required to obtain the
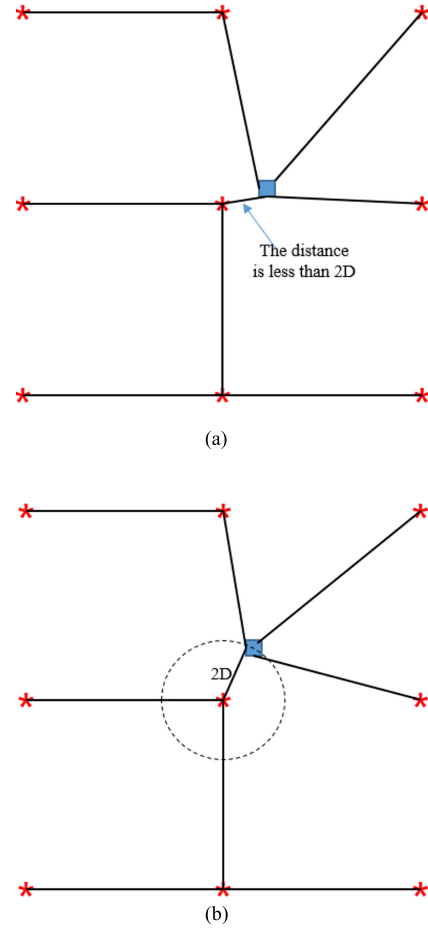
Fig. 3. (a) Initial optimized substation location that is extremely close to the WT. (b) Substation location adjustment when the initial optimized substation location is extremely close to the WT.

landowner's consent. Only then can a cable pass through the area. In addition, some restricted areas exist, such as oil wells and permafrosts, on onshore wind farms. Cables cannot pass through these areas owing to safety concerns and the high cost of construction. In other words, these areas must be bypassed. The authors in [22] and [23] introduced a mathematical method to connect two vertices. The method, which can ensure a minimum distance, was applied to wind farm cable connections in this article. The process is illustrated in Fig. 4.

As shown in Fig. 4, A and B represent two WTs on an onshore wind farm, where a restricted area exists between them. Starting from point A, two tangents of the restricted area are drawn. Subsequently, two tangential points (C and D) can be obtained. The same process was performed for point B. Tangential points (E and F) were obtained as well. The minimum distance between A and B is the shorter path in (A, C, E, B) and (A, D, F, B). Finally, the cable lays along the shorter path. The formulation is as follows:

$$D(A, B) = \min(|AC| + L_o(C, E) + |BE|,$$
$$|AD| + L_o(D, F) + |BF|). \qquad (8)$$

This article has been accepted for inclusion in a future issue of this journal. Content is final as presented, with the exception of pagination.

LI *et al.*: CABLE CONNECTION OPTIMIZATION FOR ONSHORE WIND FARMS CONSIDERING RESTRICTED AREA AND TOPOGRAPHY 5

Fig. 4. Distance calculation under restricted area.

a

b

Fig. 5. Different strategies for considering topography. (a) Install the cable on the same plane. (b) Install the cable at the same depth.

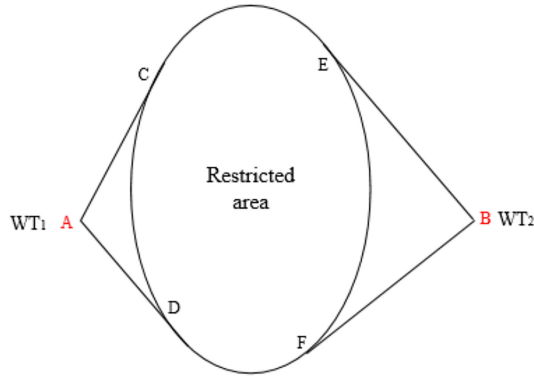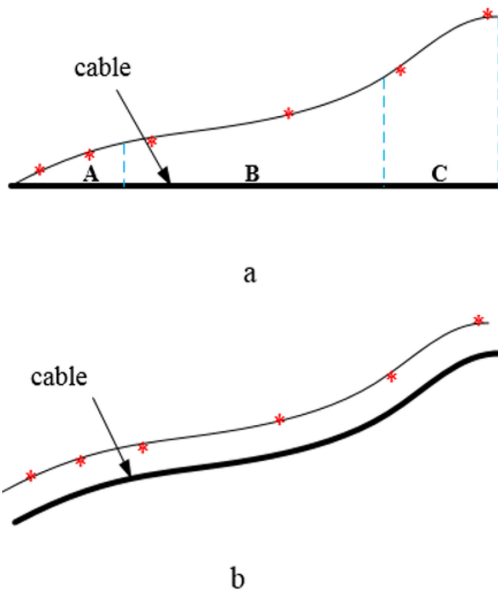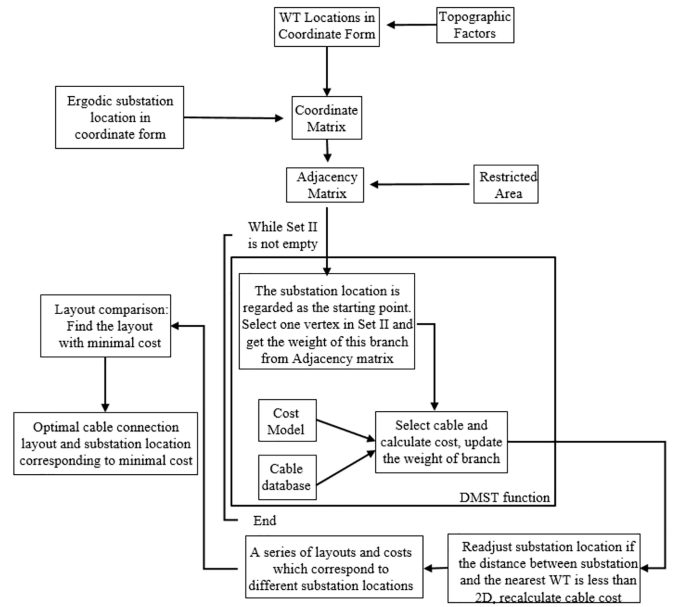Fig. 6. Optimization framework.

The effect of topography is reflected in the cable installation and maintenance costs. While the height difference between the highest and lowest positions on the onshore wind farm is large, the cost and construction difficulty of the strategy shown in Fig. 5(a), which allows cables to be buried in the same plane, are extremely high. In Fig. 5(b), the cables are buried in a fixed depth. If the installation cost is fixed at the same depth, the effect of topography is reflected in the cable length. Compared with the method in Fig. 5(b), the method in Fig. 5(a) can reduce the cable length and decrease the power loss along the cable more effectively, but the cost of cable laying is higher. In this article, the cable was laid, as shown in Fig. 5(b).

In the formulation, $L_o(p_1, p_2)$ represents the minor arc length between p_1 and p_2. The calculation steps of the shortest distance between two WTs on an onshore wind farm are as follows:
1) judge whether a restricted area exists between two WTs;
2) if it exists, then use the formulation (8);
3) if it does not exist, calculate the straight line distance between two points;

E. Effect of Topography

The construction site of an onshore wind farm may not be a flat surface. For a more accurate designed cable connection and calculated cost, topographic factors cannot be ignored. According to the altitude, the location of the wind farm can be categorized into different regions. Each region has corresponding cable installation and maintenance costs, as shown in Fig. 5(a).

In Fig. 5(a), the red spots represent the locations of WTs. The wind farm is categorized into three regions (A, B, and C). The cable connecting WTs is buried in the same plane.

F. Optimization Framework

The substation location is closely related to the wind farm cable connection layout. To obtain a reasonable result, the substation location should be confirmed together with the cable connection. The substation location was set as the starting point (as explained in Section II-B) and introduced into the calculation of the adjacency matrix. Finally, the DMST can be obtained while every WT is connected. The optimization framework for the entire process is shown in Fig. 6.

Cable database: In [24], many types of cables are reported. Suitable cross-sectional areas and voltage levels are selected according to current-carrying requirements. In this simulation, XLPE-Cu ac cables were used at 33-kV rated voltage in the CS. In addition, one 132-kV cable was used to transmit power from a substation on an onshore wind farm to a high-voltage substation.

The locations of WTs were determined in advance and were not changed. According to the topographic factors of onshore wind farms, the location of each WT can be calculated in the coordinate form. The optimal location of a substation can be obtained at a certain location on the wind farm. Every time a

This article has been accepted for inclusion in a future issue of this journal. Content is final as presented, with the exception of pagination.

6   IEEE SYSTEMS JOURNAL

TABLE I
INTRODUCTION OF CABLE COLOR

CS				
Voltage Level	33KV			
Type	AC			
Color	Blue	Green	Magenta	Yellow	Black
Cable sectional area, mm^2	70	95	150	240	400
		120	185	300	500

(a)

(b)

Fig. 7.   (a) Regular wind farm. (b) Irregular wind farm.

new substation location is added, the new substation location will participate in the operation of the DMST's main function. It is noteworthy that a new coordinate matrix that includes the coordinates of the substation and WTs will be produced. Based on the coordinate matrix and restricted area, the adjacency matrix, including the distance between two locations, will be generated. These distances are used as the weights of the branches. Subsequently, the cable connection layout of the CS will be confirmed in the DMST function based on the principle introduced in Section II-C. The length of the selected branches and the number of WTs behind every branch will be recorded. Owing to the current-carrying capacity limitation, the quantity and types of cables in every branch must be selected appropriately. All cable information used is shown in Table I. It is assumed that all WTs are operated at the rated power. While the number of WTs after each branch is being determined, the cable selection of the corresponding branch can be confirmed. Subsequently, the total cable cost can be calculated using (1)–(3), and the distance between the substation location and nearest WT is assessed. If the distance thereof is less than 2D, then the substation location should be readjusted, as described in Section III-D, and the cable cost recalculated. The process does not end until Set II becomes empty. Finally, a series of costs and layouts corresponding to different substation locations can be obtained.

The optimal cable connection layout should be selected from the results of the layout comparison. Eventually, the optimal cable connection layout and substation location can be obtained.

III. CASE STUDY

The simulation was performed on the MATLAB software platform. An irregular and a regular wind farm were selected as the research object to illustrate the effects of the restricted area and topography on onshore wind farms.

In total, there were 48 WTs on the regular wind farm and 80 WTs on the irregular wind farm. The selected WT configuration was Vestas V90-2.0 MW (90-m rotor diameter) [25]. For a more concrete conclusion, a regular and an irregular wind farm were selected in the case study. These two wind farms were on a slope of angle 5°. The layouts of the regular and irregular wind farms are shown in Fig. 7(a) and (b), respectively. The red dots in Fig. 7 represent the WTs. Detailed WT coordinates and the high-voltage substation location are provided in Tables IV and V
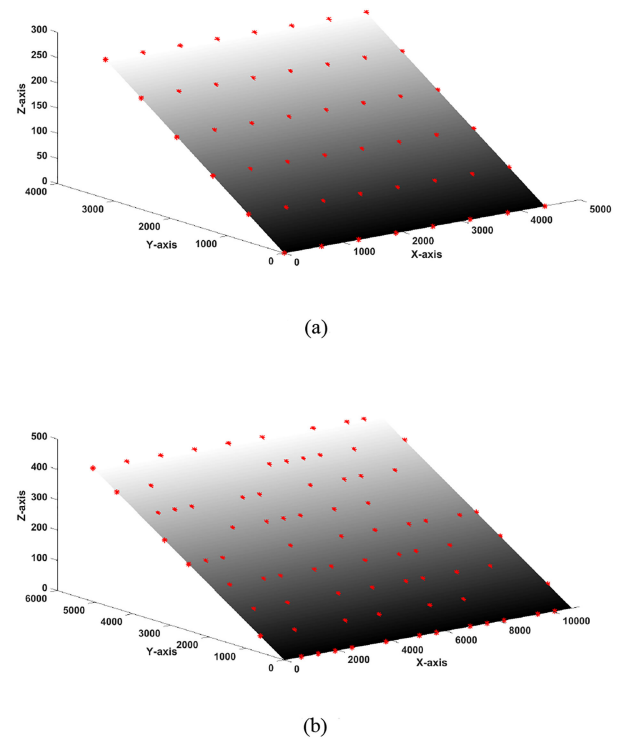
in the Appendix, respectively. To ensure the safe operation of the WTs and capture sufficient wind energy, the minimum distance between the WTs is generally set to seven rotor diameters [26]. This article focuses on the topology design of the CS. Therefore, it is assumed that the WT layout introduced in Fig. 7 is optimal.

A. Introduction of Wind Farm

In Fig. 7, the red dots indicate the locations of WTs. The algorithm used in the cable connection is the DMST. After all the power generated by the WTs has been transferred into the substation and adjusted to the appropriate voltage, the power is transmitted from a substation to a high-voltage substation through a transmission cable. The voltage levels in the CS and TS are 33 and 132 kV, respectively. Three scenarios in each study case were selected to elaborate the further optimization of the cable connection in the restricted area and the topographic factors. To demonstrate the necessity of the considered factors and for a fair comparison between the scenarios studied, we applied the following limitations and assumptions in this article.

1) The locations of the WTs and high-voltage substation are fixed during the entire optimization process.
2) All WTs on the onshore wind farm are operating at the rated power.
3) Only one substation will gather the generated power of the WTs on the onshore wind farm. The capacity of this substation in regular wind farm is 400 MVA and can accommodate 48 WTs. The capacity of this substation in irregular wind farm is 800 MVA and can accommodate 80 WTs.

This article has been accepted for inclusion in a future issue of this journal. Content is final as presented, with the exception of pagination.

LI *et al.*: CABLE CONNECTION OPTIMIZATION FOR ONSHORE WIND FARMS CONSIDERING RESTRICTED AREA AND TOPOGRAPHY

7

4) The submarine cables used have a small possibility of failure (approximately 0.001/km/year) [27]. The environment of cables on onshore wind farms is better than that on offshore wind farms. This implies that the possibility of failure on onshore wind farms is less; therefore, cable reliability is not considered.

5) No parallel HVAC lines is required in the transmission line.

6) The substation location must be determined on onshore wind farms.

7) The algorithm used in the scenarios is the DMST.

B. Regular Wind Farm

Scenario I: CS Cable Layout Without Considering Restricted Area and Topographic Factors.

This scenario serves as a comparison of the impact of topography and restricted area on cable connection layout. In this scenario, the cable connection layout is optimized without considering restricted area and topographic factors. The different color lines represent different types of cables, as explained in Table I. The green square indicates the location of the substation in the wind farm. By using the optimization procedure, the cable connection layout can be obtained as Fig. 8(a).

Scenario II: CS Cable Layout Without Considering Topographic Factors.

Occasionally, not all land can be used on a wind farm. In this scenario, the restricted area is considered when optimizing the cable connection layout. The gray triangle indicates the rock area. Because of the highly complex construction and the high cost of cable installation, cables typically do not pass through this area. Therefore, the cable layout is as shown in Fig. 8(b).

Scenario III: Optimal CS Cable Layout Considering Restricted Area and Topographic Factors.

In this scenario, the optimal CS cable connection layout can be obtained by the optimization framework shown in Fig. 6. Compared with Scenario II, Scenario III additionally considers the topography in the optimization process. Although the wind farm is relatively flat, the cable connection may be more suitable for an actual wind farm construction by considering both the topographic factors and restricted area. The connection layout is illustrated in Fig. 8(c).

The distance between the substation and the WT in Scenario III is extremely small; therefore, the final result must be readjusted. The adjusted cable connection is shown in Fig. 8(d).

Comparison: Not all areas can be used on a wind farm owing to a number of constraints. A comparison of Fig. 8(a) and (b) shows that the restricted area affects the substation location significantly, as shown by (2.8, 0.8, 0.07) in Fig. 8(a) and (3.10, 0.59, 0.05) in Fig. 8(b). The topology of the CS changed markedly owing to the restricted area. As mentioned in Section III-A, the wind farm is on a slope. Although the slope angle is only 5°, the topography should be considered in the design process to obtain a more suitable cable connection structure. It is clear that Fig. 8(b) and (c) differ vastly in terms of cable selection and cable topology. For the case of the restricted area, Table II shows that the total cable cost of Scenario III is

Fig. 8. (a) CS cable layout in regular wind farm without considering restricted area and topographic factors. (b) CS cable layout in regular wind farm without considering topographic factors. (c) CS cable layout in regular wind farm considering restricted area and topographic factors. (d) Adjusted CS cable layout in regular wind farm considering restricted area and topographic factors.

lower than that of Scenario II. Meanwhile, the total cable cost in Scenario III is reduced by 2.86% compared with Scenario II. The investment in TS cables is reduced by only 0.02 MDKK. This is because the substation location of Scenario II barely changed compared with that of Scenario III. However, the topology and cable selection of the CS changed significantly, as shown in Fig. 8. Therefore, the CS cable cost is reduced by 1.41 MDKK, which indicates an excellent optimization. It is noteworthy that the CS cable length of Scenario III is only 40 m shorter than that of Scenario II. However, the final CS cable cost is reduced significantly. This shows that the cable selection affects the cable investment significantly, thereby necessitating topology

TABLE II
INTO CABLE LAYOUT COMPARISON IN REGULAR WIND FARM

Regular wind farm	Scenario I	Scenario II	Scenario III	Scenario III(adjusted)
CS cable length (km)	29.57	30.01	29.97	29.98
TS cable length (km)	5.31	5.14	5.13	5.13
CS cable cost (MDkk)	31.75	37.11	35.70	35.83
TS cable cost (MDkk)	13.28	12.85	12.83	12.83
Total cable cost (MDkk)	45.03	49.96	48.53	48.66
Substation location (km)	(2.8, 0.8, 0.07)	(3.10, 0.59, 0.05)	(3.11, 0.60, 0.05)	(3.0, 0.54, 0.04)
Distance between substation and nearest WT (m)	327.7	64.2	50.0	180

optimization. However, the distance between the substation and nearest WT in Scenario III is 50 m, which is less than the minimum safe operating distance (2D). Therefore, the substation location should be adjusted in the manner introduced in Section II-D. The final adjusted substation location is (3.0, 0.54, 0.04). By comparing Fig. 8(c) and (d), it is clear that the adjusted substation location only affects the length of the cable that is directly connected to it. The types of cables in the CS and the length of cables not directly connected to the substation are not affected. Scenario III (adjusted) is reduced by 2.60% compared with Scenario II. The cables in Scenario III (adjusted) cost slightly higher than those in Scenario III but satisfy the safety requirements.

C. Irregular Wind Farm

For a more concrete final conclusion, the irregular wind farm was used as the simulation object. The simulation was based on the following three scenarios. Fig. 9(a), (b), and (c) represent Scenarios I, II, and III, respectively. In Fig. 9, the gray rectangle and circle represent the restricted area. Different color lines represent different cable, as shown in Table I. Due to the large number of WTs in the irregular wind farm, there may be more than one cable between two WTs. The dotted line in the Fig. 8 represents two cables.
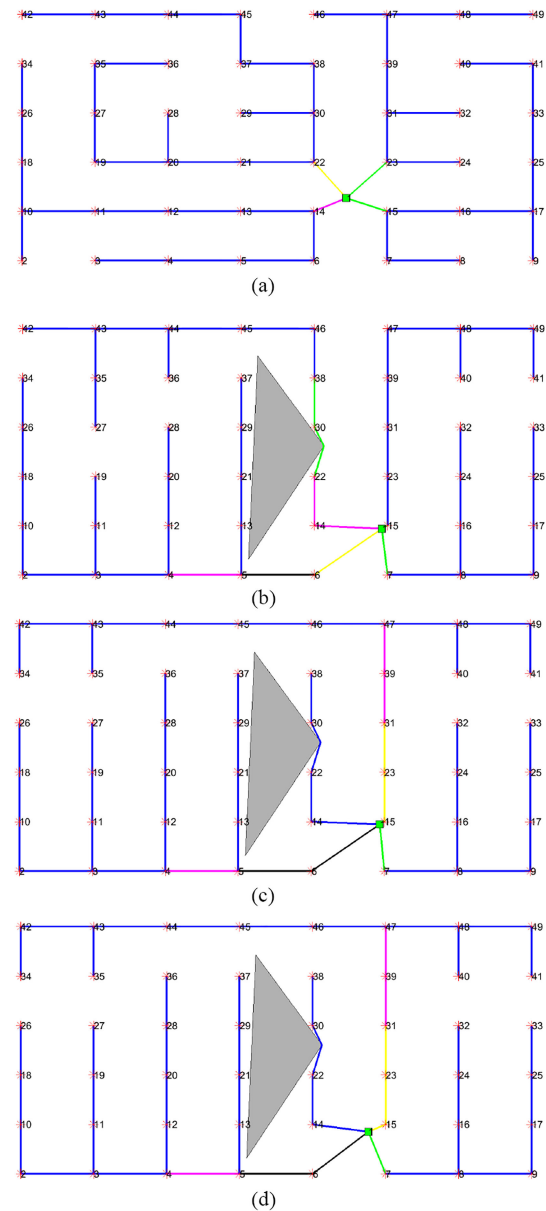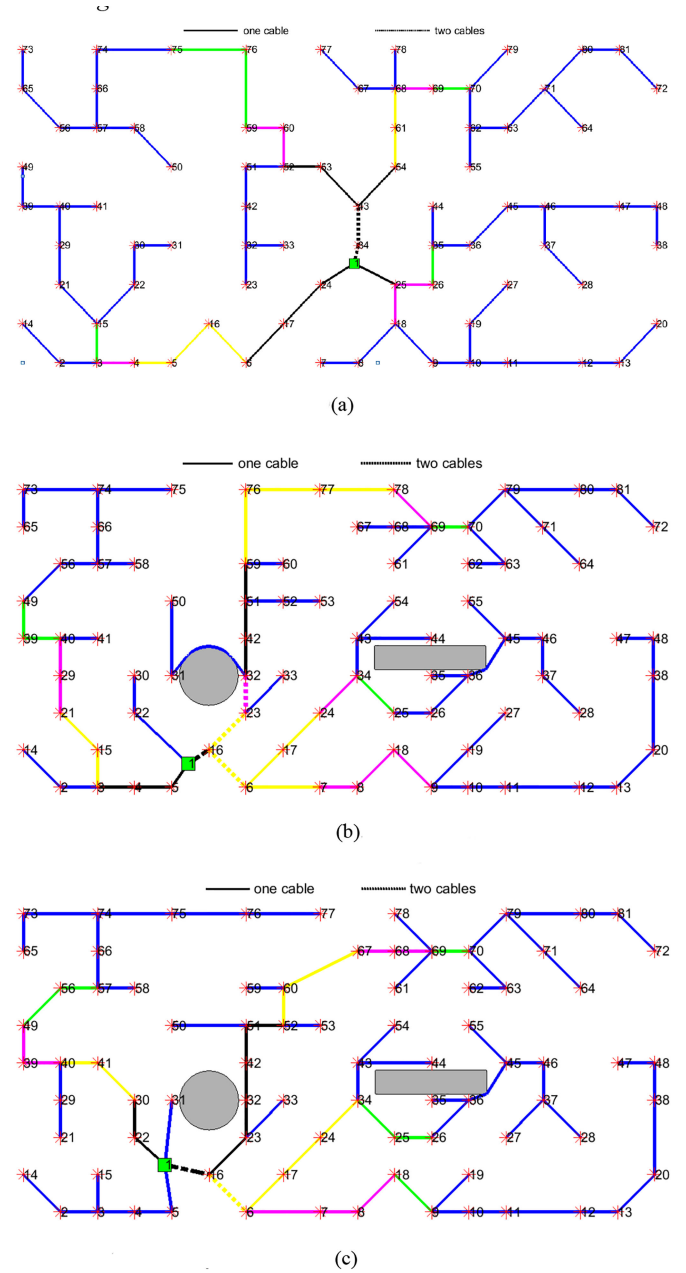

Fig. 9. (a) CS cable layout in irregular wind farm without considering restricted area and topographic factors. (b) CS cable layout in irregular wind farm without considering topographic factors. (c) CS cable layout in irregular wind farm considering restricted area and topographic factors.

Scenario I: CS Cable Layout Without Considering Restricted Area and Topographic Factors.

Scenario II: CS Cable Layout Without Considering Topographic Factors.

Scenario III: The Optimal CS Cable Layout Considering Restricted Area and Topographic Factors.

The distance between the substation and WT in Scenario III is larger than 2D. Therefore, the substation location need not be adjusted.

TABLE III
CABLE LAYOUT COMPARISON IN IRREGULAR WIND FARM

Irregular wind farm	Scenario I	Scenario II	Scenario III
CS cable length (km)	60.44	69.89	68.52
TS cable length (km)	11.60	10.71	11.19
CS cable cost (MDkk)	92.85	107.86	103.88
TS cable cost (MDkk)	34.80	32.13	33.57
Total cable cost (MDkk)	127.65	139.99	137.45
Substation location (km)	(5.6, 1.6, 0.14)	(2.8, 0.4, 0.03)	(2.4, 0.8, 0.06)
Distance between substation and nearest WT (m)	293.7	310.2	670.1

TABLE IV
COORDINATES OF WT AND HIGH-VOLTAGE SUBSTATION
IN REGULAR WIND FARM

	(X, Y, Z)		(X, Y, Z)
High-voltage	(2200,-2000,0)	25	(4410, 1260, 110.2)
Substation		26	(0, 1890, 165.3)
2	(0, 0, 0)	27	(630, 1890, 165.3)
3	(630, 0, 0)	28	(1260, 1890, 165.3)
4	(1260, 0,0)	29	(1890, 1890, 165.3)
5	(1890, 0, 0)	30	(2520, 1890, 165.3)
6	(2520, 0, 0)	31	(3150, 1890, 165.3)
7	(3150, 0, 0)	32	(3780, 1890, 165.3)
8	(3780, 0, 0)	33	(4410, 1890, 165.3)
9	(4410, 0, 0)	34	(0, 2520, 220.4)
10	(0, 630, 55.1)	35	(630, 2520, 220.4)
11	(630, 630, 55.1)	36	(1260, 2520, 220.4)
12	(1260, 630, 55.1)	37	(1890, 2520, 220.4)
13	(1890, 630, 55.1)	38	(2520, 2520, 220.4)
14	(2520, 630, 55.1)	39	(3150, 2520, 220.4)
15	(3150, 630, 55.1)	40	(3780, 2520, 220.4)
16	(3780, 630, 55.1)	41	(4410, 2520, 220.4)
17	(4410, 630, 55.1)	42	(0, 3150, 275.5)
18	(0, 1260, 110.2)	43	(630, 3150, 275.5)
19	(630, 1260,110.2)	44	(1260, 3150, 275.5)
20	(1260, 1260, 110.2)	45	(1890, 3150, 275.5)
21	(1890, 1260, 110.2)	46	(2520, 3150, 275.5)
22	(2520, 1260, 110.2)	47	(3150, 3150, 275.5)
23	(3150, 1260, 110.2)	48	(3780, 3150, 275.5)
24	(3780, 1260, 110.2)	49	(4410, 3150, 275.5)

Comparison: By comparing Fig. 9(a) and (b), it is clear that the restricted area affects the substation location considerably. Table III also reflects this situation, i.e., the substation location is (5.6, 1.6, 0.14) in Scenario I and (2.8, 0.4, 0.03) in Scenario II. After considering the effect of the restricted area, the effect of topography on the substation location appears insignificant, similar to (2.8, 0.4, 0.03) location in Scenario II and (2.4, 0.8, 0.06) location in Scenario III. However, the topography imposes a significantly effect on the final cable investment. The total cable cost in Scenario III is reduced by 1.81% compared with Scenario II. The investments in the CS cable costs decreased by 3.98 MDKK significantly. This is because the cable connection topology and corresponding cable selection changed when the topography is considered.

IV. CONCLUSION AND FUTURE WORK

This article is the first to apply the DMST algorithm to optimize the cable connection of onshore wind farms when considering the restricted area and topography. Through the study of a regular and an irregular wind farm, it was discovered that the restricted area affected the determination of the substation location significantly. The cable connection topology and corresponding cable selection changed significantly because of the topography. In the DMST algorithm optimization process, the cable cross-sectional area and voltage level should be selected appropriately to satisfy the current-carrying capacity and minimize the cable cost. In addition, the substation location should be adjusted when the distance between the substation location and WT is extremely small to affect the safe operation of onshore wind farms. Under the conditions of safe operation, the total cable cost in a regular wind farm is decreased while considering the restricted area and topography. Meanwhile, for the irregular wind farm, the total cable cost is also reduced. This indicates

that the restricted area and topography must be considered in the optimization process to obtain a more economical CS topology.

In the future, energy losses should be considered as an optimization condition. The optimal number of substations can be determined by comparing the different costs of the CS corresponding to various numbers of substations on wind farms.

APPENDIX

The coordinates of each WT and high-voltage substation in regular wind farm are shown in Table IV.

The coordinates of each WT and high-voltage substation in irregular wind farm are shown in Table V.

This article has been accepted for inclusion in a future issue of this journal. Content is final as presented, with the exception of pagination.

10   IEEE SYSTEMS JOURNAL

TABLE V
COORDINATES OF WT AND HIGH-VOLTAGE SUBSTATION
IN IRREGULAR WIND FARM

	(X, Y, Z)		(X, Y, Z)
High-voltage Substation	(5305,-10000,0)	41	(1260, 2520, 220.4)
		42	(3780, 2520, 220.4)
2	(630, 0, 0)	43	(5670, 2520, 220.4)
3	(1260, 0, 0)	44	(6930, 2520, 220.4)
4	(1890, 0, 0)	45	(8190, 2520, 220.4)
5	(2520, 0, 0)	46	(8820, 2520, 220.4)
6	(3780, 0, 0)	47	(10080, 2520, 220.4)
7	(5040, 0, 0)	48	(10710, 2520, 220.4)
8	(5670, 0, 0)	49	(0, 3150, 275.5)
9	(6930, 0, 0)	50	(2520 3150, 275.5)
10	(7560, 0, 0)	51	(3780 3150, 275.5)
11	(8190, 0, 0)	52	(4410 3150, 275.5)
12	(9450, 0, 0)	53	(5040 3150, 275.5)
13	(10080, 0, 0)	54	(6300 3150, 275.5)
14	(0, 630, 55.1)	55	(7560 3150, 275.5)
15	(1260, 630, 55.1)	56	(630 3780, 330.6)
16	(7560, 630, 55.1)	57	(1260 3780, 330.6)
17	(3150, 630, 55.1)	58	(1890 3780, 330.6)
18	(4410, 630, 55.1)	59	(3780 3780, 330.6)
19	(6300, 630, 55.1)	60	(4410 3780, 330.6)
20	(10710, 1260, 55.1)	61	(6300 3780, 330.6)
21	(630, 1260, 110.2)	62	(7560 3780, 330.6)
22	(1890, 1260, 110.2)	63	(8190 3780, 330.6)
23	(3780, 1260, 110.2)	64	(9450 3780, 330.6)
24	(5040, 1260, 110.2)	65	(0 4410, 385.7)
25	(6300, 1260, 110.2)	66	(1260 4410, 385.7)
26	(6930, 1260, 110.2)	67	(5670 4410, 385.7)
27	(8190, 1260, 110.2)	68	(6300 4410, 385.7)
28	(9450, 1260, 110.2)	69	(6930 4410, 385.7)
29	(630, 1890, 165.3)	70	(7560 4410, 385.7)
30	(1890, 1890, 165.3)	71	(8820 4410, 385.7)
31	(2520, 1890, 165.3)	72	(10710 4410, 385.7)
32	(3780, 1890, 165.3)	73	(0, 5040, 440.8)
33	(4410, 1890, 165.3)	74	(1260, 5040, 440.8)
34	(5670, 1890, 165.3)	75	(2520, 5040, 440.8)
35	(6930, 1890, 165.3)	76	(3780, 5040, 440.8)
36	(7560, 1890, 165.3)	77	(5040, 5040, 440.8)
37	(8820, 1890, 165.3)	78	(6300, 5040, 440.8)
38	(10710, 1890, 165.3)	79	(8190, 5040, 440.8)
39	(0, 2520, 220.4)	80	(9450, 5040, 440.8)
40	(630, 2520, 220.4)	81	(10080, 5040, 440.8)

REFERENCES

[1] T. Soukissian, "Use of multi-parameter distributions for offshore wind speed modeling: The Johnson S_B distribution," *Appl. Energy*, vol. 111, pp. 982–1000, 2013.

[2] N. Ederer, "The market value and impact of offshore wind on the electricity spot market: Evidence from Germany," *Appl. Energy*, vol. 154, pp. 805–814, 2015.

[3] G. Shi, X. Cai, C. Sun, Y. Chang, and R. Yang, "All-DC offshore wind farm with parallel connection: An overview," in *Proc. 12th IET Int. Conf. AC DC Power Transmiss.*, 2016, p. 75–75.

[4] N. Wang, J. Li, W. Hu, B. Zhang, Q. Huang, and Z. Chen., "Optimal reactive power dispatch of a full-scale converter based wind farm considering loss minimization," *Renewable Energy*, vol. 139, pp. 292–301, Aug. 2019.

[5] M. Zhao, Z. Chen, and F. Blaabjerg, "Optimization of electrical system for a large DC offshore wind farm by genetic algorithm," in *Proc. NORPIE*, Jun. 2004, pp. 14–16.

[6] H. Ling-Ling, C. Ning, Z. Hongyue, and F. Yang, "Optimization of large-scale offshore wind farm electrical collection systems based on improved FCM," in *Proc. Int. Conf. Sustain. Power Gener. Supply*, 2012, pp. 1–6.

[7] A. M. Jenkins, M. Scutariu, and K. S. Smith, "Offshore wind farm inter-array cable layout," in *Proc. IEEE Grenoble Conf.*, 2013, pp. 1–6.

[8] F. M. Gonzalez-Longatt, P. Wall, P. Regulski, and V. Terzija, "Optimal electric network design for a large offshore wind farm based on a modified genetic algorithm approach," *IEEE Syst. J.*, vol. 6, no. 1, pp. 164–172, Mar. 2012.

[9] S. Houria, A. Rezak, and M. Abdellah, "Optimal Design of the electric connection of a wind farm," *Energy*, vol. 165, pp. 972–983, Dec. 2018.

[10] J. Bauer and L. Lysgaard "The offshore wind farm array cable layout problem—A planar open vehicle routing problem," *J. Oper. Res. Soc.*, vol. 66, no. 3, pp. 360–368, 2015.

[11] P. Hou, W. Hu, and Z. Chen, "Offshore substation locating in wind farms based on prim algorithm," in *Proc. Power Energy Soc. General Meeting*, 2015, pp. 1–5.

[12] P. Hou, W. Hu, C. Chen, and Z. Chen, "Optimization of offshore wind farm cable connection layout considering levelised production cost using dynamic minimum spanning tree algorithm," *IET Renewable Power Gener.*, vol. 10, no. 2, pp. 175–183, 2016.

[13] M. Banzo and A Ramos, "Stochastic optimization model for electric power system planning of offshore wind farms," *IEEE Trans. Power Syst.*, vol. 26, no. 3, pp. 1338–1348, Aug. 2011.

[14] S. Lumbreras and A. Ramos "Optimal design of the electrical layout of an offshore wind farm applying decomposition strategies," *IEEE Trans. Power Syst.*, vol. 28, no. 2, pp. 1434–1441, May 2013.

[15] A. C. Pillai, J. Chick, L. Johanning, and V. de Laleu, "Offshore wind farm electrical cable layout optimization," *Eng. Optim.*, vol. 47, no. 12, pp. 1689–1708, 2015.

[16] L. Chen and E. Macdonald, "A system-level cost-of-energy wind farm layout optimization with landowner modeling," *Energy Convers. Manage.*, vol. 77, no. 1, pp. 484–494, 2014.

[17] P. Hou, W. Hu, C. Chen, M. Soltani, and Z. Chen, "Optimization of offshore wind farm layout in restricted zones," *Energy*, vol. 113, pp. 487–496, 2016.

[18] S. Lundberg, "Performance comparison of wind park configurations," Chalmers Univ. Technol., Goteborg, Sweden, Tech. Rep. 30R, Aug. 2003.

[19] M. Zubiaga, G. Abad, J. A. Barrena, S. Aurtenetxea, and A. Carcar, "Evaluation and selection of AC transmission lay-outs for large offshore wind farms," in *Proc. 13th Eur. Conf. Power Electron. Appl.*, 2009, pp. 1–10.

[20] J. A. Bondy and U. S. R. Murty, "Graph theory with applications," *J. Oper. Res. Soc.*, vol. 28, no. 1, pp. 237–238, 1997.

[21] R. A. Devore and V. N. Temlyakov, "Some remarks on greedy algorithms." *Adv. Comput. Math.*, vol. 5, no. 1, pp. 173–187, 1996.

[22] M. de Berg, M. Van Kreveld, M. Overmars, and O. C. Schwarzkopf, "Visibility graphs," in *Computational Geometry*. Berlin, Heidelberg: Springer, 2000.

[23] S. K. Ghosh and D. M. Mount, "An output sensitive algorithm for computing visibility graphs," in *Proc. 28th Ann. Symp. Found. Comput. Sci.*, Los Angeles, CA, USA, 1987, pp. 11–19.

[24] ABB corporation, "XLPE submarine cable systems attachment to XLPE land cable systems-user's guide," 2013.

[25] "General SPECIFICATION V90-1.8/2.9 MW 50 Hz VCS," Vestas Technol. R&D, Aarhus, Denmark, Nov. 19, 2010.

[26] O. Dahmani, S. Bourguet, M. Machmoum, P. Guerin, P. Rhein, and L. Josse, "Optimization of the connection topology of an offshore wind farm network," *IEEE Syst. J.*, vol. 9, no. 4, pp. 1519–1528, Dec. 2015.

[27] C. Kamalakannan *et al.*, "Power electronics and renewable energy systems," in *Proc. Power Eng. Soc. Summer Meeting*, 2015, pp. 1263–1264.

Qi Huang (Senior Member, IEEE) was born in Guizhou, China. He received the B.S. degree in electrical engineering from Fuzhou University, Fuzhou, China, in 1996, the M.S. degree from Tsinghua University, Beijing, China, in 1999, and the Ph.D. degree from Arizona State University, Tempe, AZ, USA, in 2003.

He is currently a Professor with the University of Electronics Science and Technology of China (UESTC), Chengdu, China, the Head of the School of Mechanical and Electrical Engineering, UESTC, and the Director of the Sichuan State Provincial Laboratory of Power System Wide-Area Measurement and Control. His current research and academic interests include power system instrumentation, power system monitoring and control, and power system high-performance computing.

Junxian Li received the B.S. degree in automation from Hohai University, Nanjing, China, in 2017. He is currently working toward the M.S. degree in electric engineering with the University of Electronic Science and Technology of China, Chengdu, China.

Zhou Liu (Senior Member, IEEE) received the Ph.D. degree in energy technology from Aalborg University, Aalborg, Denmark, in 2013.

Since December 2014, he has been a Postdoc Researcher with the Department of Electrical Power Engineer, Norwegian University of Science and Technology, Trondheim, Norway. From 2017 to 2018, he was a Postdoc Fellow with the Department of Electrical Sustainable Energy, TU Delft, Delft, The Netherlands. He is currently an Assistant Professor with the Department of Energy Technology, Aalborg University. His main research interests include power system protection, power system stability and control, energy system integration, digital substation, and smart grid technology.

Weihao Hu (Senior Member, IEEE) received the B.Eng. and M.Sc. degrees in electrical engineering from Xi'an Jiaotong University, Xi'an, China, in 2004 and 2007, respectively, and the Ph.D. degree from Aalborg University, Aalborg, Denmark, in 2012.

He is currently a Full Professor and the Director of the Institute of Smart Power and Energy Systems, University of Electronics Science and Technology of China, Chengdu, China. He was an Associate Professor with the Department of Energy Technology, Aalborg University and the Vice Program Leader of Wind Power System Research Program with the same department. He has led/participated in more than 10 national and international research projects and he has more than 160 publications in his technical field. His research interests include intelligent energy systems and renewable power generation.

Prof. Hu is an Associate Editor for IET Renewable Power Generation, the Guest Editor-in-Chief for the *Journal of Modern Power Systems and Clean Energy* Special Issue on Applications of Artificial Intelligence in Modern Power Systems, the Guest Editor-in-Chief for the *Transactions of China Electrical Technology* special issue on planning and operation of multiple renewable energy complementary power generation systems, and the Guest Editor for the IEEE TRANSACTIONS ON POWER SYSTEM special section on enabling very high penetration renewable energy integration into future power systems. He was serving as the Technical Program Chair (TPC) for IEEE Innovative Smart Grid Technologies (ISGT) Asia 2019 and was serving as Secretary and Treasurer of Power and Energy Society Chapter, IEEE Denmark Section. He is currently serving as Chair for IEEE Chengdu Section PELS Chapter.

Cong Chen received the M.Math. degree from Cambridge University, Cambridge, U.K., in 2010, and the Ph.D. degree from the University of Leeds, Leeds, U.K., in 2014.

He is currently a Senior Data Scientist with the Health Data Insight and Public Health England, Cambridge, U.K., working in cancer surveillance and epidemiology.

Zhe Chen (Fellow, IEEE) received the B.Eng. and M.Sc. degrees from the Northeast China Institute of Electric Power Engineering, Jilin City, China, in 1982 and 1986, respectively, and the Ph.D. degree from the University of Durham, Durham, U.K., in 1997

He is currently a Full Professor with the Department of Energy Technology, Aalborg University, Aalborg, Denmark. He is also the Leader of Wind Power System Research Program with the Department of Energy Technology, Aalborg University and the Danish Principle Investigator for Wind Energy of Sino-Danish Centre for Education and Research. He has led many research projects and has more than 400 publications in his technical field. His research areas include power systems, power electronics and electric machines; and his main current research interests include wind energy and modern power systems.

Dr. Chen is an Editor for the IEEE TRANSACTIONS ON POWER SYSTEMS, an Associate Editor for the IEEE TRANSACTIONS ON POWER ELECTRONICS, a Fellow of the Institution of Engineering and Technology, London, U.K., and a Chartered Engineer in the U.K.

Xiawei Wu received the B.S. and M.S. degrees in electrical engineering in 2015 and 2017, respectively, from the University of Electronic Science and Technology of China, Chengdu, China, where he is currently working toward the Ph.D. degree in control science and engineering.